SPECTROMETER-BASED MAGNETOGRAPHS

HARRISON P. JONES
NASA/Goddard Space Flight Center, Laboratory for Astronomy and Solar Physics, Southwest Solar Station, c/o NSO, PO Box 26732, Tucson, AZ, 85726

ABSTRACT   The techniques and instrumentation for inferring magnetic fields using a spectrometer or spectrograph rather than a narrow-band filter are reviewed. With array detectors and/or Fourier transform spectroscopy, the polarimetric data is acquired over the relevant spectral range strictly simultaneously with no possibility of spatial misregistration. Several recent examples of spectrometer-based magnetographs are discussed and compared, and new observations from the NASA/NSO Spectromagnetograph of magnetic flux, velocity field, continuum intensity, equivalent width, and line depth in active regions and the whole sun are shown.

INTRODUCTION

In the preceding review, Professor Ai (1993) aptly summarizes the evolution of magnetographs and emphasizes the growing use and sophistication of narrow-band filters and video detector systems culminating in his optical design for a filter to produce simultaneous images in a number of contiguous narrow-band wavelength channels (Ai, 1991). This paper is intended to complement that presentation by summarizing the use and promise of more traditional spectrometers for solar magnetography.

The principles for using a spectrograph to detect solar magnetic fields as developed by Hale (1908), Babcock (1953), and others have been widely applied in the construction and operation of a number of magnetographs around the world. Recent technological improvements in telescopes, polarimetry, detectors, and data systems have stimulated development of a new generation of such instruments, many of which are in early stages of operation or in final stages of development. These magnetographs are all complicated with many unusual or unique features whose discussion would be far beyond the scope of this paper. Indeed, better descriptions of many such instruments, along with new data from them, can be found in other papers in these proceedings. Instead, the distinguishing features of spectrometer-based instruments will be discussed in general terms and will be illustrated with a specific example of a new instrument. Finally, some future directions for the development of magnetographs will be discussed.

WHY A SPECTROMETER?

In the typical Babcock configuration, the spectrograph is basically used as a filter to isolate one or two wavelength bands on the wings of a spectrum line, and spatial information at any instant is available at best only along a linear segment of the solar surface. In the early stages of filter development, the spectrograph's low cost, easy tunability, and very high underlying spectral resolution made it a viable competitor as a monochromator. Moreover, the photomultiplier tubes which have been the detectors for most Babcock-type magnetographs are efficient, nearly linear, and have high dynamic range.

Vestiges of these advantages remain today in that the wavelength domain available to spectrographs and detectors exceeds that obtainable from a single narrow-band filter, and the comparative sensitivity and linearity of photomultiplier tubes is still high. However, universal filters can now be constructed which can be tuned to different spectrum lines over a reasonably broad spectral range even more rapidly than a grating; which have ample spectral resolution; and which have the substantial advantage of transmitting two-dimensional spatial information without degradation by image scanning. Moreover, clever implementation and increasing quality of two-dimensional detectors has largely vitiated the advantages of single photomultiplier tubes.

A spectrometer still enjoys one key advantage which will be the primary focus of this paper; with a suitable detector, the intensity can be recorded strictly simultaneously over the entire wavelength domain of interest (e.g., a spectrum line). Seeing distortions during a single exposure are unavoidable in a ground-based instrument but are at least uniform across the spectral domain when a spectrometer is used. Thus physical information can be derived with maximal reliability from the recorded Stokes profiles without fear of differential contamination by seeing or solar temporal variations for exposures at different wavelengths. In contrast, current filtergraphs must be sequentially tuned to obtain spectra and practical limits on exposure times and detector readout require "destretching" of images at each wavelength to compensate for seeing variations. A problem of great importance but beyond the scope of this paper is to quantify and compare the compromises between spatial, spectral, and temporal domains for both types of instruments as they are used in practice.

Table I compares how current spectrometer-based magnetographs span and resolve the spatial-spectral domain since this is the critical feature to compare with filter-based instruments. Columns from left to right identify the observatory and, where appropriate, instrument; full-disk (F) or active-region (A) field of view (FOV); number of pixels in wavelength and space; spectral (Å) × spatial (arc seconds) pixel size; and Stokes parameters measured. Note that approximate typical values are given for parameters in many instances since they may often be changed according to, for example, choice of spectrum line, detector, optical train, or observing target. Full-sun instruments which do not ordinarily resolve active regions are not listed in Table I. Acronyms are expanded as follows: FTS–Fourier Transform Spectrometer; SPMG—Spectromagnetograph; NIM—Near Infrared Magnetograph; HAO—High Altitude Observatory; ASP—Advanced Stokes Polarimeter; VSSHG—Video Spectra-Spectroheliograph; VTT—Vacuum Tower Telescope; THEMIS—Télescope Héliographique pour l'Étude du Magnétisme et des Instabilités de l'atmosphère Solaire; SVST–Swedish Vacuum

TABLE I   Spectrometer-Based Magnetographs

Observatory	FOV	$\#\lambda \times \#x$	$\Delta\lambda(\text{Å}) \times \Delta x(\pi)$	Stokes
Nat. Solar Obs.				
Kitt Peak				
FTS	A	10000×1	0.005×4	I,Q,V
SPMG	F/A	30×512	0.035×1.1	I,V
NIM	A	128×128	0.1×0.5	I,Q,U,V
Sacramento Peak				
HAO/ASP	A	512×240	0.04×0.4	I,Q,U,V
Mees Solar Obs.	A	128×1	0.025×3	I,Q,U,V
San Fernando Obs./VSSHG	A	240×512	0.07×0.5	I,V
Mt. Wilson Obs.	F	2×1	0.065×10	I,V
Tenerife, Gregory	A	1024×1024	0.008×0.34	I,V
Tenerife, German VTT	A	1024×024	0.003×0.172	I,Q,U,V
Tenerife, THEMIS	A	288×384	0.013×0.24	I,Q,U,V
La Palma, SVST	A	240×240	0.005×0.1	I,Q,U,V
ETH, ZIMPOL	A	385×285	0.037×0.85	I,Q,U,V
Potsdam	A	6×1	0.08×3	I,Q,U,V
Ondrejov	A	1×1	0.08×4	I,V
Pulkovo	A	400×240	0.03×0.6	I,V
Crimea	A	4×1	$0.09 \times 1\text{-}15$	I,Q,U,V
Irkutsk/Sayan				
Vector Magnetograph	A	2×1	0.065×2	I,Q,U,V
Panoramic Magnetograph	A/F	2×1	0.065×2	I,V
Kodaikanal	A	Film	0.005×1.0	I,Q,U,V
Kunming/Yunnan	A	512×512	0.012×0.2	I,Q,U,V
Hida Domeless	A	512×10	$.0034 \times 0.13$	I,Q,U,V
Okayama	A	6×1	$0.027\text{-}0.080 \times 10$	I,Q,U,V

Solar Telescope; ETH—Eidgenossiche Technische Hochschule; ZIMPOL—Zurich Imaging Stokes Polarimeter.

Babcock- or Severny-type magnetographs with one or two spectral channels are in service at the Mount Wilson 150-foot Tower (Howard *et al.*, 1983, Ulrich *et al.*, 1991); Potsdam (Staude *et al.*, 1991); Ondrejov; the Crimean Astrophysical Observatory (Stepanov and Severny, 1962); Sayan (Grigoryev *et al.*, 1985; Lebedev and Grigoryev, 1977); and Okayama (Makita *et al.*, 1985). The Potsdam magnetograph (Staude *et al.*, 1991) uses three wavelength points on two independent spectrum lines. The Mees Stokes Polarimeter (Mickey, 1985) uses a linear array oriented parallel to the dispersion. The FTS at the National Solar Observatory's (NSO) McMath-Pierce facility on Kitt Peak (Stenflo *et al.*, 1983) perhaps employs the extreme compromise between spectral and spatial detection. The spectrum from just a single spatial point has extended range, very high spectral resolution, absolute wavelength calibration, and no contamination from spectral stray light. A very large and fundamental literature on the physics of the Sun's magnetic field has been based on this data (see, for example, the review by Stenflo, 1989).

The magnetographs in Table I which make full use of two-dimensional spatial-spectral detection are the NASA/NSO Spectromagnetograph (Jones *et al.*, 1992), to be discussed in more detail; the HAO/NSO Advanced Stokes Polarimeter at the Sacramento Peak Vacuum Tower Telescope (cf. Lites *et al.*, 1991, 1993); the San Fernando Observatory Video Spectra-Spectroheliograph (Chapman and Walton, 1991); the Near Infrared Magnetograph at the NSO/Kitt Peak McMath Telescope (Jaksha *et al.*, 1993); the French THEMIS instrument (Rayrole, 1991; Mein and Rayrole, 1993); the "ZIMPOL" detector systems for rapidly switching charge between masked and exposed portions of CCDs (Povel *et al.*, 1990); the new Scanning Stokes Polarimeter at the Yunnan Observatory (Ding *et al.*, 1993); the Pulkovo magnetograph (Parfinenko, 1991); and the Hida Domeless Solar Telescope (Makita *et al.*, 1991). In addition, the Swedish and German telescopes in the Canary Islands can be equipped with CCD's for operation as magnetographs under special circumstances. Some interesting results at very high spatial resolution from these telescopes are reported in other papers of these proceedings (e.g., Sanchez Almeida *et al.*, 1993; Deubner *et al.*, 1993; Lites *et al.*, 1993; Soltau, 1993) and elsewhere (e.g., Lites *et al.*, 1990). Earlier spatial-spectral photographic instruments developed by Rayrole (1967) and by Title and Andelin (1971) saw limited use because of difficulty in handling enormous quantities of film.

THE NASA/NSO SPECTROMAGNETOGRAPH

A detailed description of this new instrument which replaces the 512-channel Diode Array Magnetograph (Livingston *et al.*, 1976b) at the NSO/Kitt Peak Vacuum Telescope (Livingston *et al.*, 1976a) has recently been published elsewhere (Jones *et al.*, 1992). Briefly, an anamorphic optical system reimages long-slit spectra from the Littrow spectrograph onto a commercial CCD television camera. A video processing system separates opposite states of circular polarization from the input stream, digitizes the video input, integrates the raw data, and flat-fields the spectra. Magnetic flux, line-of-sight velocity, contin-
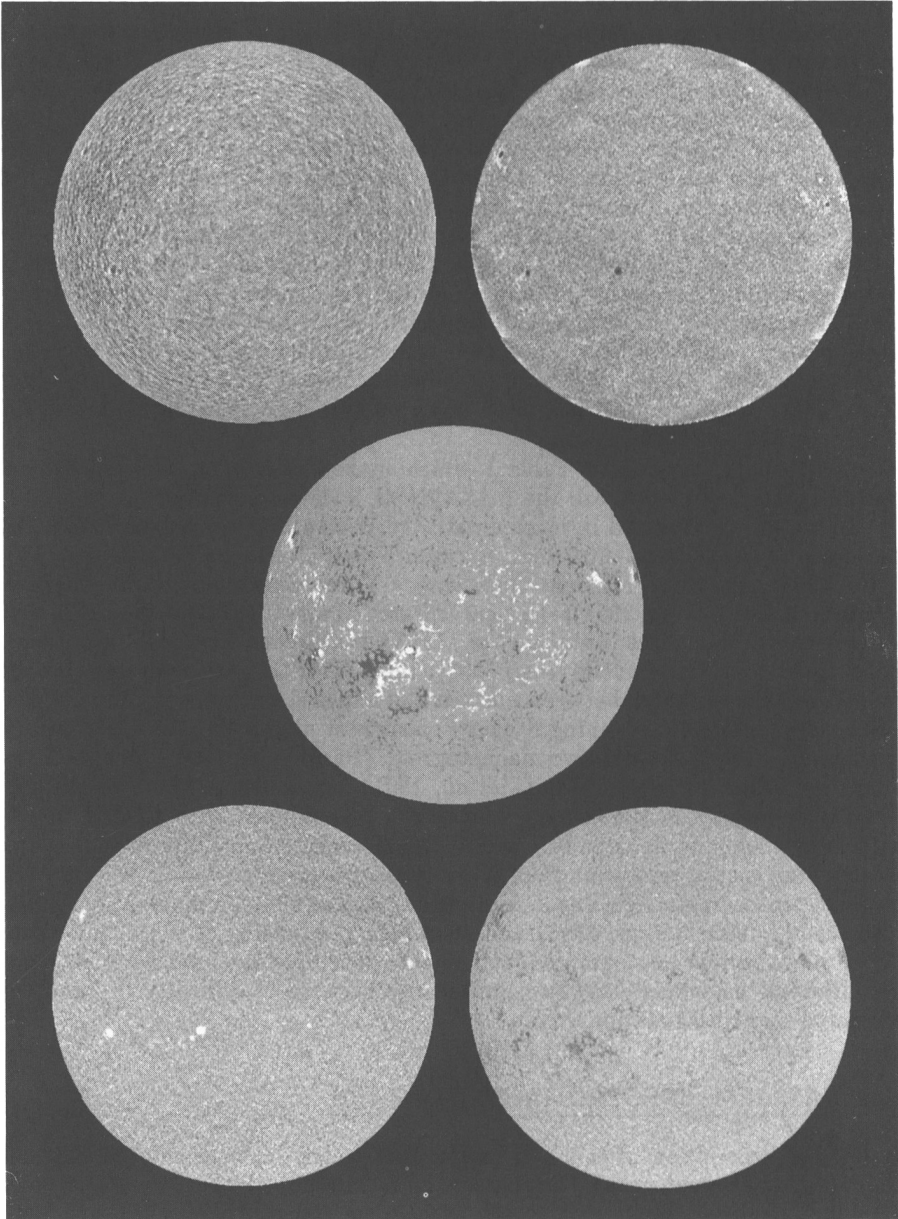
FIGURE I   Spectromagnetograph data for 14 June, 1992: velocity (upper left); continuum contrast (upper right); magnetic flux (center); equivalent width (lower left); line depth (lower right).

uum intensity, equivalent width, and line depth are calculated as the data are acquired, and the observer controls set-up and data acquisition from a workstation terminal through a specially developed software interface. To find magnetic flux, line-of-sight velocity, and central line depth, the wavelength displacement of the central minimum of the spectrum line in each state of circular polarization at every spatial point is computed by an efficient convolution algorithm which takes into account variations in the line profile. Full-disk magnetograms require about an hour when all data products are retained while active-region scans can be obtained in as little as 90 seconds but more typically require about five minutes. Spatial pixels are about 1.1 arc-seconds and spectral pixels are 30-40 mÅ for typical lines in the visible and near infrared. Since April 12, 1992, the Kitt Peak daily magnetograms have been obtained with the Spectromagnetograph. Computer hardware will be installed in the near future which will enable improved data reduction and more rapid spatial scanning.

Observations

A sample full-disk magnetogram together with the associated velocity, continuum, equivalent-width, and line-depth images are shown in Figure I. The observations were taken in the 5507 Å line of Fe I on 14 June, 1992. Quantities determined directly from measurements of line-center wavelength (magnetic and velocity field) are remarkably free of residual artifacts of fixed pattern correction or variations in sky transparency. The magnetic and velocity images are grey-scale displays of "real" time calculations with only minor cosmetic postobservation correction. The images for equivalent width and line depth show some residual fixed-pattern noise which has been largely removed by simple "destreaking" algorithms. The continuum intensity, on the other hand, requires no on-line analysis but is neither ratioed nor differenced and, since it is thus sensitive to both transparency fluctuations and optical imperfections, requires extensive off-line reduction.

Many familiar features such as Evershed flow, supergranulation, sunspot umbra and penumbra, limb faculae, etc. may be easily identified and compared on a pixel-by-pixel basis with each other and with magnetic field. Perhaps less familiar are the spatial patterns displayed in equivalent width and line depth. Areas of moderate magnetic flux (e.g., unipolar network outside of active regions) are well mapped by reduced (darker grey scale) central line depth. A similar decrease in equivalent width can be seen faintly in full-scale images and is more readily evident in statistical trends of correlation plots (cf., Jones, 1992). Spatial correlations of equivalent width with magnetic field tend to be masked by the sensitivity of the former to global oscillations (Duvall, 1992; private communication) which cannot be properly filtered from the present data due to the long acquisition time. The weakening of the absorption line in network regions together with the bright continuum appearance of such areas near the solar limbs is consistent with a simple model where the outward temperature gradient is less in the magnetic areas than in the surrounding quiet sun. Stronger plage regions near sunspots also appear dark in line depth, but the equivalent width is markedly enhanced; this suggests that the temperature-density structure is distinctly different from quiet regions in a way which increases the column density of Fe I.
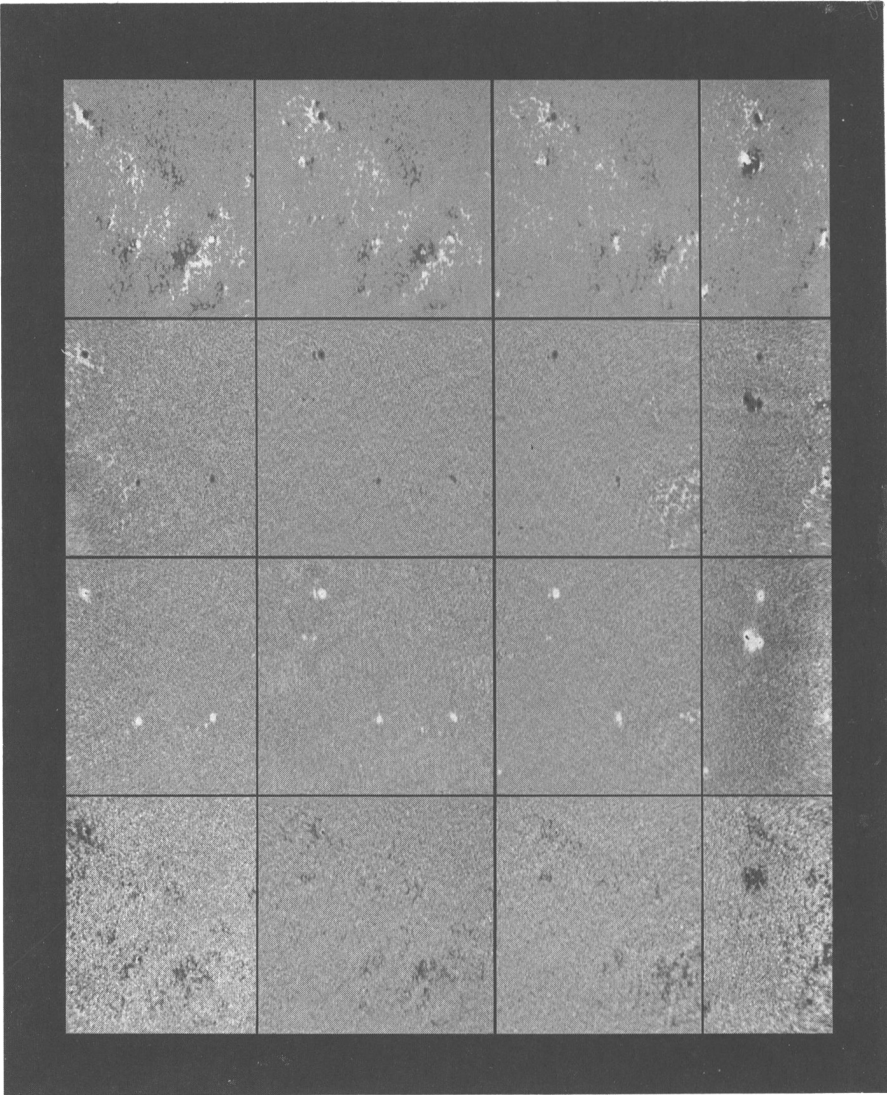
FIGURE II   Carrington projections of active region evolution. From top to bottom: magnetic field, continuum contrast, equivalent width, and line depth. From left to right: 14, 17, 20, and 23 June 1992.

A hint of how such data may be used to study the structure and evolution of active regions is shown in Figure II, which is a montage of selected images from a video presented in the oral version of this paper. The figure shows sections of full-disk data remapped as a function of solar longitude (shifted at the Carrington rotation rate without compensation for differential rotation) and sine of solar latitude. The data show the evolution of NOAA/Space Environment Laboratory active regions 7194 (lower right), 7197 (lower left) and 7201 (upper left) and span about 102 degrees in longitude and range from approximately -30 to +35 degrees in latitude. Where appropriate, the fields of view have been clipped to remove distorted areas near the limb.

The most noticeable feature is the tentative appearance and sudden rapid growth of the sunspot group (region 7205) just south of region 7201. The region is just beyond the field of view on the 14th but has a small but well-formed bipolar appearance by the 17th. The magnetic feature on the 17th is associated with a very small spot in the continuum image and a doubly peaked region of enhanced equivalent width. The feature is only weakly visible in line depth. On the 20th, the magnetic character is only slightly changed, the small spot has apparently vanished, the enhancement in equivalent width is markedly reduced, but the definition in line depth is somewhat enhanced. By the 23rd the magnetic field has markedly increased, three large spots have formed, and the signatures in both equivalent width and line depth are well formed; the other three active regions have gradually decayed and the new area dominates the field of view. Such simultaneous views of magnetic and thermal evolution of active regions on long time scales will lead to an improved view of the magnetohydrodynamic processes underlying active region growth and decay.

FUTURE DEVELOPMENTS

In the near future, many details of two-dimensional spectral polarimetry will be explored and improved. These include, for example, techniques for removing fixed pattern noise from images of spectrum lines in the presence of mild fringing, rapid digitization and readout, data storage, and on-line analysis. Even without improvement, however, there are clearly many fundamental solar problems which can now be studied with quantitative precision.

The next fundamental advance may well be the design of instruments or detectors which avoid scanning in either wavelength or space—three-dimensional multispectral imagers. Imaging Fourier Transform Spectrometers have been discussed for many years, and one such instrument has already been proposed for spacecraft operation in the "SIMURIS" (Coradini, *et al.*, 1991) mission. Promising progress has been achieved in the development of three-dimensional organic films (Keller, 1992; private communication) which, when cryogenically cooled and exposed to light, may store spectrally resolved images. Finally, Ai (1991) has presented designs for multichannel filters. However, the data acquisition, storage, reduction, and analysis capabilities of any such instrument must also keep pace with the increased dimensionality of the data stream.

As a preliminary exercise to see how feasible such a data system might be, Table II shows the approximate current cost in thousands of US dollars to scale the data and analysis system for the Spectromagnetograph to a multichannel

system of 512 x 512 spatial x n spectral points obtained simultaneously in a one-second exposure. The configuration is assumed to be as follows: one camera (2K$) and one video acquisition/processor board per channel (20K$); one target CPU (5K$), one attached processor board for flat-fielding (20K$), and one VME chassis (5K$) for every six channels; and one workstation host with disks and tapes (50K$) with two high-speed attached processors (40K$) for on-line analysis.

TABLE II   Data System for a Multispectral Imager

# Channels	Cost (K$)
8	300
16	500
32	1000
64	1800

Table II includes only the present-day cost of detectors, image processors, and computers. To include assembly and software, this cost should probably be multiplied by a factor of two to three. One should also note that the number of board-level elements at present scales for integrating electronic components is quite large which poses serious questions regarding the system's ultimate reliability. In the United States, funding a data system for more than a few channels would require very strong justification and broad community support well beyond the scope of an ordinary individual research proposal. On the other hand, a data system for the Spectromagnetograph would have been similarly costly just one or two decades ago. By the time that real optical systems for multispectral imagers can be realized, the costs for the expanded data systems which they will require may be far more manageable.

REFERENCES

Ai, G. 1991 in *Solar Polarimetry*, L. November, ed., NSO Workshop, Sunspot, NM, 113.

Ai, G. 1993, these proceedings.

Babcock, H. W. 1953, *Ap. J.* **118**, 387.

Chapman, G. A. and Walton, S. R. 1991, in *Solar Polarimetry*, L. November, ed., NSO Workshop, Sunspot, NM, 37.

Coradini, M. Damé, Foing, B. Haskell, G. Kassing, D. Olthof, H., Mersch, G., Ruutten, R. J., Thorne, A. P., and Vial, J.-C. 1991, *SIMURIS Scientific and Technical Study—Phase I.*

Deubner, F.-L., Fleck, B., Hofmann, J., and Schmidt, W. 1993, these proceedings.

Ding, Y., Xuan, J., and Qu, Z. 1993, these proceedings.

Grigoryev, V. M., Kobanov, N. I., Osak, B. F., Selivanov V. L., and Stepanov, V.E. 1985, in *Measurements of Solar Vector Magnetic Fields*, M. Hagyard, ed., NASA Conf. Pub. 2374, 231.

Hale, G. E. 1908, *Ap. J.* **28**, 315.

Howard, R. Boyden, J. E., Bruning, D. H., Clark, M. K., Crist, H. W. and Labonte, B. J. 1983, *Solar Phys.* **87**, 195.

Jaksha, D., Kopp, G., Mahaffey, C., Plymate, C., Rabin, D., and Wagner, J.: 1992, in *Proceedings, IAU Symp. 154*, D. Rabin, ed., Kluwer Academic Publishers, in press.

Jones, H. P., Duvall, T. L. Jr., Harvey, J. W., Mahaffey, C. T., Schwitters, J. D., and Simmons, J. E. 1992, *Solar Phys.*, **139**, 211.

Lebedev, N. N. and Grigoryev V. M. 1977, *Solar Phys.* **48**, 417.

Lites, B. W., Elmore, D., Murphy, G., Skumanich, A., Tomczyk, S. and Dunn, R. B. 1991, in *Solar Polarimetry*, L. November, ed., NSO Workshop, Sunspot, NM, 3.

Lites, B. W., Elmore, D. F., Tomczyk, S., Seagraves, P., Skumanich, A., and Streander, K. V. 1993, these proceedings.

Lites, B. W. Scharmer, G. B., and Skumanich, A. 1990, *Ap. J.* **355**, 329..

Makita *et al.*, 1985, *Publ. Aston. Soc. Japan* **37**, 561.

Makita, M., Funakoshi, Y., and Hanaoka, Y., 1991, in *Solar Polarimetry*, L. November, ed., NSO Workshop, Sunspot, NM, 198.

Mein, P. and Rayrole, J. 1993, these proceedings.

Mickey, D. L. 1985, *Solar Phys.* **97**, 223.

Parfinenko, L. D. 1991, *Sov. Astron.* **35**, 199.

Povel, H. P., Aebersold, H., and Stenflo, J. O. 1990, *Appl. Opt.* **29**, 1186.

Rayrole, J. 1967, *Ann. Astrophys.* **30**, 257.

Sanchez Almeida, J., Martínez Pillet, V., Trujillo Bueno, J., and Lites, B. W. 1993, these proceedings.

Soltau, D. 1993, these proceedings.

Staude J., Hofmann, A. and Bachmann, H. 1991, in *Solar Polarimetry*, L. November, ed., NSO Workshop, Sunspot, NM, 49.

Stepanov, V. E. and Severny, A. B. 1962, *Izv. Krims. Astrofiz. Obs.* **28**, 166.

Stenflo, J. O., Twerenbold, D., Harvey, J. W., Brault, J. W. 1983, *Astr. Ap. Supp.* **54**, 505.

Stenflo, J. O. 1989, *Astr. Ap. Rev.* **1**, 3.

Title, A. M. and Andelin, J. P., Jr. 1971, in *Solar Magnetic Fields*, IAU Symp. 43, R. Howard, ed., 298.

Ulrich, R. K., Webster, L., Boyden, J. E., Magnone, N., and Bogart, R. S. 1991, *Solar Phys.* **135**] 211.